HAIT Journal of Science and Engineering, Volume 1, Issue 3, pp. 528-541

Quantum Hall effects and edge states in layered disordered superconductors *

Baruch Horovitz[1,*], Victor Kagalovsky[2], and Yshai Avishai[1]

[1] *Department of Physics, and Ilze Katz Center for Nanotechnology, Ben-Gurion University of the Negev, Beer-Sheva 84105, Israel*
[2] *Negev Academic College of Engineering, Beer-Sheva 84100, Israel*
[*] *Corresponding author: hbaruch@bgumail.bgu.ac.il*
Received 24 November 2004, accepted 15 December 2004

Abstract

Layered singlet paired superconductors with disorder and broken time reversal symmetry are studied focusing on edge states and the corresponding quantum Hall effects. We find quantum Hall phases with spin Hall coefficients of $\sigma_{xy}^{spin} = 0, 2$ separated by a spin metal phase. We identify a spin metal-insulator localization exponent as well as a spin conductivity exponent of ≈ 0.96. In presence of a Zeeman term an additional $\sigma_{xy}^{spin} = 1$ phase appears. The phase diagram, in terms of the average intergrain transmission and the interlayer tunneling, demonstrates charge-spin separation in transport.

PACS: 73.20.Fz, 72.15.Rn, 73.43.-f

1 Introduction

The problem of quasiparticle transport and localization in disordered superconductors is of considerable interest in view of experimental activity on the high T_c cuprates as well as theoretical realization that disordered superconductors provide new symmetry classes of random matrix theory [1].

*Presented at Research Workshop of the Israel Science Foundation *Correlated Electrons at High Magnetic Fields*, Ein-Gedi/Holon, Israel, 19-23 December 2004

Of particular interest is class C for which the Hamiltonian breaks time reversal symmetry but spin rotation invariance remains intact. Physically, it can be realized in materials consisting of singlet superconductor grains in a magnetic field or else, by a superconductor in the absence of magnetic field whose order parameter breaks time reversal invariance, such as $d+id'$. Class C can therefore be realized by high T_c compounds where d wave pairing is well established. In fact, $d+id'$ pairing has been suggested [2], in particular in overdoped compounds or as field induced [3].

Transport properties of random superconductors are unusual since a quasiparticle does not carry charge, being screened by the condensate, while the singlet paired condensate does not transport spin. Furthermore, the gapless nature of d wave pairing with low lying quasiparticle excitations leads to a rich phase diagram in 2-dimensions (2D) with spin quantum Hall phases [4, 5], spin insulators and spin metals [6, 7]; a metallic phase was also found for triplet pairing [8].

In Section 2 we study edge states of d+id' superconductors and show their relation with quantum Hall effects (QHE). The description with edge states allows also to identify the intergrain transmission, which is an essential parameter of the network model. In Section 3 and 4 we present the network model in 2D and 3-dimensions [9] (3D), respectively, and the resulting phase diagrams.

2 Edge states

An important insight into the nature of $d+id'$ superconductors comes from studying their edge states [2, 3, 10] which provide a realization of our network model and identify its parameters. In the d wave case a prominent zero bias anomaly [2, 3] has identified a surface state at zero energy. The $d+id'$ case allows current carrying chiral states that split the zero bias anomaly as seen in the overdoped compounds [3]. The chirality of these edge states leads directly to quantized Hall conductance [5, 10].

In Fig. 1 we demonstrate edge states on a 110 surface. Note that in the absence of the d' component the order parameter $\Delta(\zeta) = \Delta \sin 2\zeta$ has the symmetry $\Delta(\zeta) = -\Delta(-\zeta)$. Hence under a specular reflection a quasiparticle incident at an angle ζ and reflected at $-\zeta$ sees an order parameter that changes sign, which is a well known condition for a zero energy bound state at a SNS junction. The eigenfunctions with momentum k_y parallel to the surface, $k_y = k_F \sin\zeta$ with k_F the Fermi wavevector, are [10]

$$\psi(\zeta; x) \sim e^{-x|\sin\zeta|/\xi} \tag{1}$$

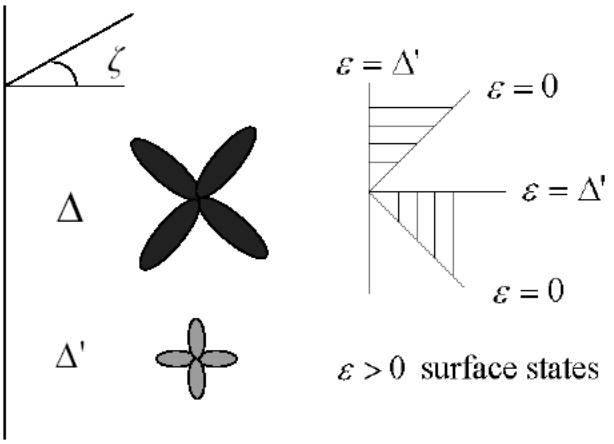

Figure 1: Order parameters of a d wave and d' wave superconductor relative to a 110 surface. Also shown is the range of incident angles which produces a bound state with positive energy.

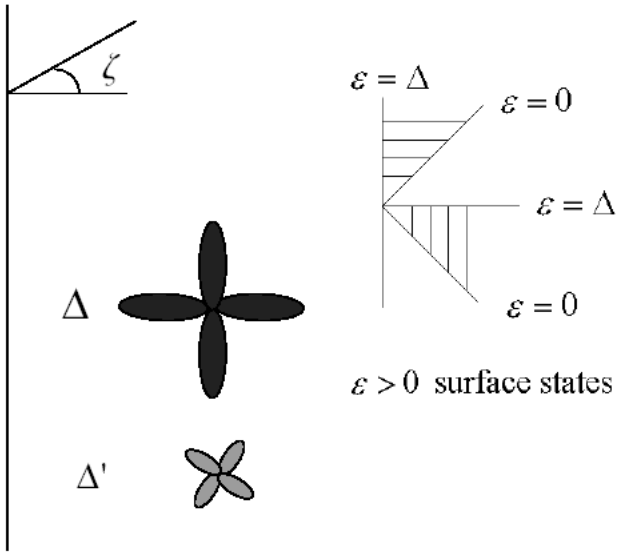

Figure 2: Order parameters of a d wave and d' wave superconductor relative to a 100 surface. Also shown the range of incident angles which produces a bound state with positive energy.

where x is a coordinate perpendicular to the surface and ξ is the coherence length associated with the Δ order parameter, $\xi = v_F/\Delta$ with v_F the Fermi velocity. Since all bound states are at energy $\epsilon = 0$ this results in a "giant" zero bias anomaly, as indeed seen in tunneling data [2, 3]. Once a Δ' order appears (we consider $\Delta' \ll \Delta$) the order parameter is $\Delta(\zeta) = \Delta \sin 2\zeta + i\Delta' \cos 2\zeta$ and it changes sign with $\zeta \to -\zeta$ only for $\zeta = \pi/4$. Hence the spectrum of bound states is in the range $0 < \epsilon < \Delta'$ for the angles as shown in Fig. 1 with $\epsilon = 0$ at $\zeta = \pm\pi/4$.

In Fig. 2 we demonstrate edge states on a 110 surface. The order parameter is $\Delta(\zeta) = \Delta' \sin 2\zeta + i\Delta \cos 2\zeta$ and the bound states are

$$\psi(\zeta; x) \sim e^{-x|\sin\zeta|/\xi'} \tag{2}$$

where $\xi' = v_F/\Delta'$. These bound states exist only for $\Delta' \neq 0$ and the spectra is in the range $0 < \epsilon < \Delta$. This energy range is mostly above the bulk gap of Δ', however, for a given k_y the surface state energy is above the corresponding one in the bulk, hence for a pure system it is stable.

Data on overdoped YBCO [3] has shown splitting in tunneling maxima even without an external magnetic field. This is consistent with the onset of $d + id'$, though $d + is$ is also possible. Further data on spontaneous magnetization [11] supports the $d+id'$ state, though final assignment awaits further data.

These edge states are chiral, reflecting the broken time reversal symmetry of the order parameter. For linear response we can linearize the spectrum near the $\epsilon = 0$ states at $\zeta = \pm\pi/4$, with velocity [10] $v' = \sqrt{8}\Delta'/k_F$ (for a (110) surface). These two branches can be represented by a spinor $\Psi^\dagger(y) = [\eta_1(y), \eta_2(y)]$ and the effective Hamiltonian in the presence of impurities has then the form [10]

$$\mathcal{H} = \int dy \Psi(y)[-iv\partial_y + V(y)\sigma_1]\Psi(y)\,. \tag{3}$$

The random potential $V(y)$ is ineffective for chiral fermions. Formally one can perform a gauge transformation

$$\Psi(y) \to \exp[i\sigma_1 \int^y V(y')dy']\Psi(y) \tag{4}$$

so that $V(y)$ cancels in the Hamiltonian. More physically, the chiral states cannot backscatter as there are no states with opposite velocity, hence they are not sensitive to impurities. For small grains a backscattering is possible between opposite edges, as studied in Section 3.

The chiral edge states imply directly QHE. We note first that there is no charge transport, since the condensate screens the motion of charge by quasiparticles. The charge hall conductance has been evaluated [10] for finite frequency ω and wavevector q with the result

$$\sigma_{xy}(\mathbf{q},\omega) = \frac{e^2}{4\pi\hbar}\frac{c_s^2 q^2}{c_s^2 q^2 - \omega^2}\,\mathrm{sign}(\Delta\Delta') \tag{5}$$

and $c_s = v_F/\sqrt{2}$. Note the appearance of a Goldstone mode in this transverse response. For standard transport one has $q \to 0$ first so that $\sigma_{xy} = 0$.

The condensate does not screen spin or heat transport. Hence by applying a spin voltage V_s, an analog of a space dependent Zeeman term $V_s = \mu_B \frac{\partial B_z}{\partial y}$, we can induce a spin current. If we define $\hbar/2$ as the unit spin conduction, in analogy to e for charge transport, then the analog of e^2/h is $(\hbar/2)^2/h = \hbar/8\pi$ and the quantized Hall conductance becomes [5]

$$\sigma_{xy}^{spin} = 2\frac{\hbar}{8\pi}\,\mathrm{sign}(\Delta\Delta') \tag{6}$$

with the factor 2 representing the two edge state channels.

Similarly, heat conduction is the ideal metal conduction, leading to thermal Hall conduction K_{xy} with the ratio K_{xy}/T being quantized

$$K_{xy} = 2\pi^2 k_B^2/3h\,. \tag{7}$$

We conclude this section by deriving the transmission between grains, a parameter which eventually controls the phase diagrams in Sections 3 and 4. Consider then two grains of $d + id'$ superconductors with parallel edge states along an axis y. An impurity provides an intergrain scattering potential $Va\delta(y)$, where a is a lattice constant. The right and left moving edge state $\psi_R(y)$ and $\psi_L(y)$ then satisfy

$$\begin{aligned} -iv\partial_x\psi_R(y) + Va\delta(y)\psi_L(x) &= E\psi_R(y) \\ iv\partial_y\psi_L(y) + Va\delta(y)\psi_R(y) &= E\psi_L(y) \end{aligned} \tag{8}$$

where E is an energy eigenvalue. Here v is the edge state velocity, $v \approx a\Delta'$ for a (110) surface and $v \approx a\Delta$ for a (100) surface [10]. The transmission from an incoming $\psi_R(y)$ to an outgoing $\psi_L(y)$ is readily evaluated as

$$T_0 = \frac{4(Va/2v)^2}{[1 + (Va/2v)^2]^2}\,. \tag{9}$$

Note that T_0 has a maximum of 1 at $Va/2v = 1$ and decreases at large V [since then the matching of states near the impurity ($E \approx \pm V$) with

the nearest levels on the edges ($E \approx \pm v/a$) is reduced]. The transmission needed for exhibiting an extended state, $T_0 = 1/2$, is achieved at $V \approx \Delta'$ for (110) edges or $V \approx \Delta$ for (100) edges, i.e. a much weaker impurity in the former case.

3 2D random superconductors

Consider a superconducting order parameter for the pairing of electrons on site i and site j, $\Delta_{ij} \sim \langle c_{i\uparrow} c_{j\downarrow} \rangle$.

A singlet supeconductor satisfies the general symmetry

$$\Delta_{ij} \sim \langle c_{i\uparrow} c_{j\downarrow} \rangle = -\langle c_{i\downarrow} c_{j\uparrow} \rangle = \langle c_{j\uparrow} c_{i\downarrow} \rangle \tag{10}$$

so that $\Delta_{ij} = \Delta_{ji}$ is symmetric. The hamiltonian, in particle-hole space is then written in the form

$$\mathcal{H}_s = \sum_{ij} \begin{pmatrix} c_{i\uparrow}^\dagger & c_{i\downarrow} \end{pmatrix} \begin{pmatrix} h_{ij} & \Delta_{ij} \\ \Delta_{ij}^* & -h_{ij}^T \end{pmatrix} \begin{pmatrix} c_{j\uparrow} \\ c_{j\downarrow}^\dagger \end{pmatrix} \tag{11}$$

where $c_{i\uparrow}, c_{i\downarrow}$ are annihilation operators for spin up or down, respectively, at site i and h_{ij} are the normal state Hamiltonian including tunneling elements between sites i, j and possibly a magnetic field; h_{ij} and Δ_{ij} may be random. This Hamiltonian has an exact symmetry under the operator

$$Q = \begin{pmatrix} 0 & 1 \\ -1 & 0 \end{pmatrix} \times \text{complex conjugation} \tag{12}$$

so that $Q\mathcal{H}_s Q^{-1} = -\mathcal{H}_s$. This corresponds to particle-hole symmetry so that the spectrum is symmetric around zero energy. This symmetry leads to a distinct classification in random matrix theories, which for the present s wave superconductors is termed class C by Altland and Zirnbauer [1]. For the network model, the transfer matrix T along a link (Fig. 3) is equivalent to an evolution in time τ (note the unidirectional propagation at each link) hence $T = \exp(-i\mathcal{H}_s\tau)$ and $QTQ^{-1} = T$. This identifies T as elements of the SU(2) group, chosen at random (with the Haar measure) to represent the randomness of the superconducting grains.

Thus T represents Andreev scattering where particles and holes are mixed. Hence quasiparticle charge in a superconductor is not conserved and the localization problem of interest in a disordered superconductor involves spin and energy transport, rather than charge transport.

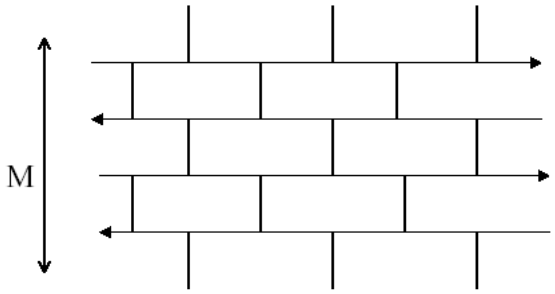

Figure 3: Network model. The links (horizontal full lines) represent propagation around superconducting grains, while nodes (vertical dotted lines) represent particle or hole transfer between grains

The nodes of the network model (vertical dotted lines in Fig. 3) correspond to transfer of either particles or holes between grains. To preserve SU(2) symmetry the latter transmissions are equal and are parameterized by a transmission $T_0 = 1/[1 + \exp(-\pi\epsilon)]$. The point $\epsilon = 0$ where transmission and reflection equal is expected to be a critical point [12]. We allow also for breaking of SU(2) symmetry by a parameter Δ which breaks the particle-hole symmetry on the nodes, i.e. the transmissions of the particle and hole are

$$T_0^e(\Delta) = T_0^{h*}(-\Delta) = 1/\{1 + \exp[-\pi(\epsilon + \Delta)]\}\,. \tag{13}$$

We proceed to present numerical studies for strips of width M and length $L \approx 10^4$, i.e. the transfer matrices are of size $M \times M$ and are multiplied L times. The eigenvalues of $T^\dagger T$ are well known to have eigenvalues of the form $\exp(-2\lambda_n L)$ where λ_n are Lyapunov exponents. The localization length is the longest scale $\xi_M = 1/\lambda_1$. The behavior of ξ_M/M identifies the type of phase: (i) ξ_M/M decreasing with M is a spin insulator, (ii) ξ_M/M independent of M is a critical state, and (iii) ξ_M/M increasing with M is a spin metal. The latter identification will be shown below by considering directly the spin conductance.

We find the scaling behavior

$$\frac{\xi_M}{M} = f(\epsilon^\nu M, \Delta^\mu M) \tag{14}$$

with $\nu \approx 1.1$ and $\mu \approx 1.4$, close to results from an exact mapping [13, 14] with $\nu = 4/3$ and $\mu = 3/2$.

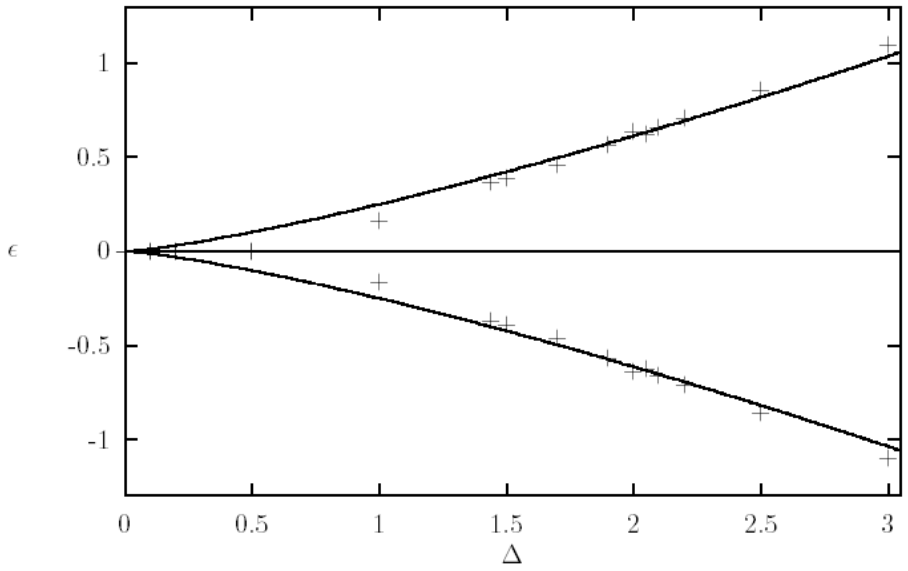

Figure 4: 2D phase diagram showing 3 phases with quantum Hall coefficients of 2,1,0.

Fig. 4 shows the phase diagram. For SU(2) symmetry with $\Delta = 0$ there is a single critical point at $\epsilon = 0$; for $\epsilon < 0$ the system has high transmission and is equivalent to the pure case as studied above, i.e. a Hall coefficient of 2. At $\epsilon > 0$ the disorder dominates and the Hall coefficient drops to 0. When $\Delta \neq 0$ there are 3 phases, with Hall coefficients $2, 1, 0$, respectively, and the phase boundaries satisfy $\epsilon_c \sim \pm\Delta^{\mu/\nu}$ with the crossover exponent of $\mu/\nu \approx 1.3$. For $\Delta \neq 0$ the symmetry reduces to U(1) with the exponent of the usual QHE, i.e. $\nu_0 \approx 2.5$ with

$$\frac{\xi_M}{M} = g[(\epsilon - \epsilon_c)^{\nu_0} M] \,. \tag{15}$$

We note that charge transport in random superconductors is determined by different parameters, i.e. it is determined by the condensate and therefore by random Josephson phases between grains. This lead to an XY model with random phase shifts which at 2D has an order-disorder transition at a finite value of disorder [15]. i.e. the phase correlation between grains is lost at high disorder. In contrast, the spin (or heat) transport is carried by quasiparticles and is determined by the average value of the transmission between grains $T_0(\epsilon)$, while disorder in ϵ is irrelevant [9]. Therefore,

although the quasiparticles are repeatedly scattered by the condensate random order parameter, spin-charge separation in transport persists on long scales. We conclude then that a superconductor-insulator transition for charge transport is disconnected from that of quasiparticle spin transport, realizing spin-charge separation in transport.

4 3D random superconductors

We extend our network model to 3D by using a layered system with additional nodes, coupling t between layers, as shown in Fig. 5, similar to the extension of the usual QHE to 3D [16].

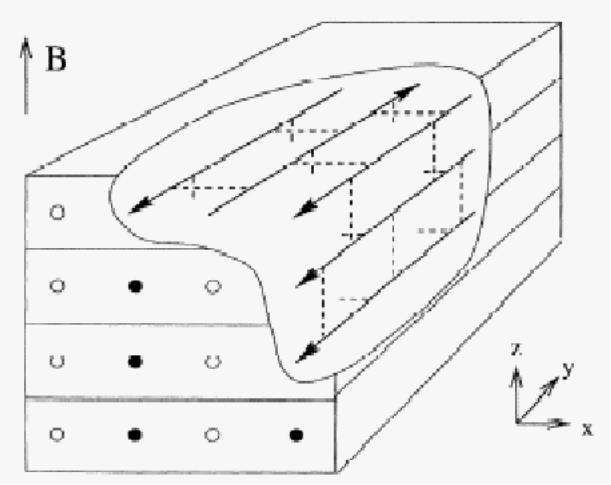

Figure 5: 3d network model following Ref. [16]. There are additional nodes (vertical dashed lines) between layers of strength t.

The transfer matrix at the node connecting neighboring layers is

$$\mathbf{T}_3 = \begin{pmatrix} \sqrt{1-t^2} & t \\ -t & \sqrt{1-t^2} \end{pmatrix} . \tag{16}$$

The transfer matrix transfers now $M \times M$ links and is of size $2M^2 \times 2M^2$. The phase diagram for the class C network model (with $\Delta = 0$) is displayed in Fig. 6. Square boxes represent critical $\epsilon_{cr}(t)$ lines. The particle-hole symmetry of the superconductor ensures a degeneracy at the critical point $\epsilon = t = 0$, i.e. the Hall coefficient changes by two units. Furthermore, in

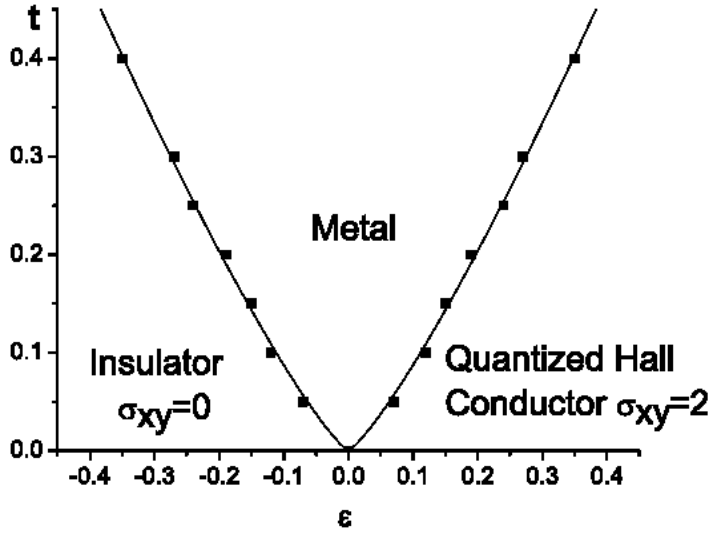

Figure 6: Phase diagram of the 3D network model with spin-rotational symmetry.

the clean limit the Hall conductance has two units as shown in Section 2, corresponding to a transmission $T_0 = 1$, i.e. $\epsilon > 0$ is large. Hence there are three distinct phases: Hall insulator with Hall conductance $\sigma_{xy} = 0$, spin metallic phase, and a quantized spin Hall phase with $\sigma_{xy} = 2$.

The width $W(t)$ in ϵ of the metallic region increases with t, and is expected to behave as[16] $W(t) \sim t^{1/\nu_{2d}}$ where ν_{2d} is the localization length exponent in 2D. The argument is that for a 2D isolated layer the mean level spacing is $\sim 1/\xi_{2d}^2$ with ξ_{2d} the 2D localization length. The states in each layer are concentrated along a percolation cluster of length ξ_{2d} and width of the edge state (a coherence length[10]) , i.e. normalized as $\sim \xi_{2d}^{-1/2}$; the interlayer coupling is then $\sim t/\xi_{2d}$. At the mobility edge the mean level spacing is of the same order as the interlayer coupling according to the Thouless criterion, hence $\epsilon \sim t^{1/\nu_{2d}}$. The curve in Fig. 6. represents the least square fit for the data, producing $W \sim t^{1/1.2}$, which is in good agreement with our value of ν_{2d} in Section 3.

The divergence of the localization length at $\epsilon_{cr}(t)$ identifies the localization exponent of a spin insulator-metal transition in 3D. We have evaluated the critical exponent at the symmetric point $t = 1/\sqrt{2}$ (larger t maps into a smaller t by rearranging layer indices) and found $\nu_{3d} = 0.96$ on both the

insulator and metal sides, as shown in Fig. 7; the same value is found for $t = 0.1$.

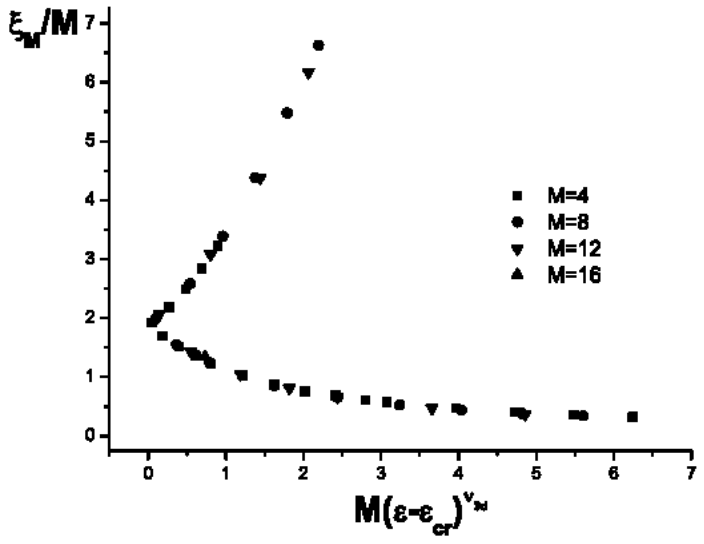

Figure 7: Scaling of renormalized localization length for the 3D network model with spin-rotational symmetry at $t = 1/\sqrt{2}$ showing an exponent $\nu_{3d} = 0.91$. The lower and upper branches correspond to the insulating $\epsilon > \epsilon_{cr}$ and metallic $\epsilon < \epsilon_{cr}$ phases, respectively.

Fig. 7 shows that in the metallic phase ξ_M/M increases approximately linearly with M. It was proposed [17] that this identifies the 3D conductivity as $\sigma_{xx} \sim (\epsilon - \epsilon_{cr})^{\nu_{3d}}$. This derivation needs to be revised since in the 3D limit the conductivity involves many Lyapunov exponents λ_n. The multichannel conductance is given by [18, 19] $g = \sum_n [1+\cosh(\lambda_n L)]^{-1}$. For a few channels $M^2 \ll L$ the lowest Lyapunov dominates, but in the 3D limit $M^2 \gg L$ the number of terms N_{eff} that contribute to g is large. In fact, for many channels the rigidity in the spectrum of $T^\dagger T$ suppresses fluctuations in $\{\lambda_n\}$ and one expects [19] $\lambda_n = n\lambda_1$. Hence $g \approx N_{eff} \approx 1/(\lambda_1 L)$. The conductance has then the form

$$g \approx N_{eff} \approx \frac{M}{L}[a(\epsilon - \epsilon_{cr})^{\nu_{3d}} M + b]\,. \tag{17}$$

This shows that the conductivity in 3D is indeed $\sigma_{xx} \equiv gL/M^2 \sim (\epsilon - \epsilon_{cr})^{\nu_{3d}}$.

On the critical line $\epsilon = \epsilon_{cr}$ the conductance is limited to the surface area and is $\sim b$.

Consider next the $\Delta \neq 0$ case with broken spin rotation symmetry. At $\Delta = 2$, e.g., the 2D system ($t = 0$) is critical at $\epsilon_{cr} = \pm 0.64$ with a critical exponent $\nu_{QH} \approx 2.5$ of the usual quantum Hall system. At $t \neq 0$, we expect each of the critical states to split into two with a band of metallic states between them (as for $\Delta = 0$), however it is not obvious wether the two internal critical curves merge or do not cross as t increases. We find merging of these lines, producing a four-phase diagram as shown in Fig. 8. Both outer critical lines scale as $t \sim |\epsilon - \epsilon_{cr}|^{\nu_{QH}}$ in agreement with the argument above. The inner curve is affected by both critical points and therefore deviates from this scaling form.

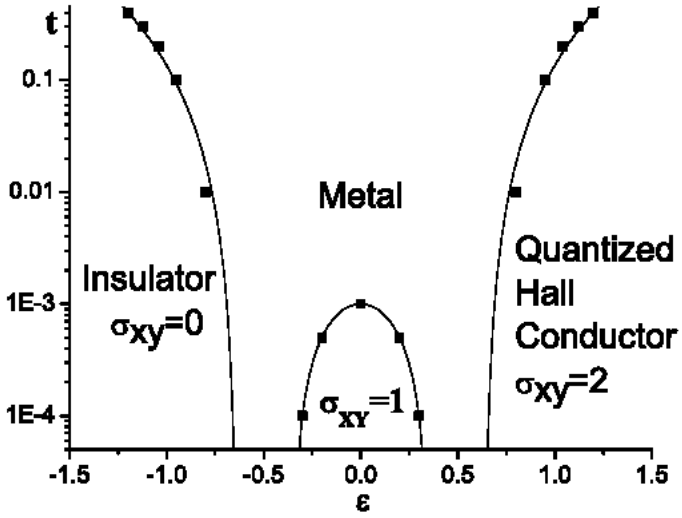

Figure 8: Phase diagram of the 3D network model with $\Delta = 2$ showing an additional phase with $\sigma_{xy} = 1$.

Fig. 8 shows the existence of a new phase with $\sigma_{xy} = 1$ which becomes metallic at very low values of t, e.g. $t = 0.001$ at $\epsilon = 0$. This feature can be traced to the rather large ξ_M/M values for $t = 0$ in the range $-\epsilon_{cr} < \epsilon < \epsilon_{cr}$. We note that at $t = 0$ a single spin state becomes extended at ϵ_{cr}, while the other spin state becomes extended independently at $-\epsilon_{cr}$. For $t < 0.001$ these extended states produce two metallic bands which do not overlap, hence when the chemical potential is in between these bands the $\sigma_{xy} = 1$

phase emerges. When $t > 0.001$ these bands overlap and a $\sigma_{xy} = 1$ phase is not possible. We emphasize that there is a single metallic phase, hence in this phase the two extended spin states mix via interlayer coupling, unlike the situation at $t = 0$.

5 Conclusions

We have demonstrated spin-charge separation in transport: spin transport and related quantum Hall transitions are controlled by the average intergrain transmission while charge transport and superconducting correlations are controlled by the amount of disorder in the intergrain Josephson coupling. We show that interlayer coupling leads to a new spin metal phase and identify the localization exponent for the spin insulator-metal transition as $\nu_{3d} \approx 0.96$. The latter is also the spin conductivity exponent when approaching the transition from the metallic side. The close relationship of QHE and edge states allows the latter to be a sensitive probe for d+id' symmetry and the corresponding QHE.

References

[1] A. Altland and M.R. Zirnbauer, Phys. Rev. B **55**, 1142 (1997); M.R. Zirnbauer, J. Math. Phys. **37,** 4986 (1996)

[2] M. Covington, M. Aprili, E. Paraoanu, L.H. Greene, F. Xu, J. Zhu, and C.A. Mirkin, Phys. Rev. Lett. **79**, 277 (1997).

[3] Y. Dagan and G. Deutscher, Phys. Rev. Lett. **87**, 177004 (2001).

[4] V. Kagalovsky, B. Horovitz, Y. Avishai, and J.T. Chalker, Phys. Rev. Lett. **82**, 3516 (1999).

[5] T. Senthil, J.B. Marston and M.P.A. Fisher, Phys. Rev. B **60**, 4245 (1999).

[6] T. Senthil, M.P.A. Fisher, L. Balents and C. Nayak, Phys. Rev. Lett. **81**, 4704 (1998).

[7] R. Bundschuh, C. Cassanello, D. Serban and M. R. Zirnbauer, Phys. Rev. B **59**, 4382 (1999).

[8] J. T. Chalker, N. Read, V. Kagalovsky, B. Horovitz, Y. Avishai, and A.W.W. Ludwig, Phys. Rev. B **65**, 012506 (2001).

[9] V. Kagalovsky, B. Horovitz, and Y. Avishai, Phys. Rev. Lett. (in press).

[10] B. Horovitz and A. Golub, Europhys. Lett. **57**, 892 (2002); Phys. Rev. B **68**, 214503 (2003).

[11] R. Carmi, E. Polturak, G. Korn, and A. Auerbach, Nature **404**, 853 (2000).

[12] J.T. Chalker and P.D. Coddington, J. Phys. C **21**, 2665 (1988)

[13] I.A. Gruzberg, A.W.W. Ludwig and N. Read, Phys. Rev. Lett. **82**, 4524 (1999).

[14] E.J. Beamond, J. Cardy and J.T. Chalker, Phys. Rev. B **65**, 214301 (2002).

[15] D. Carpentier and P. Le Doussal, Phys. Rev. Lett. **81**, 2558 (1998); B. Horovitz and P. Le Doussal, Phys. Rev. Lett. **84**, 5395 (2000).

[16] J.T. Chalker and A. Dohmen, Phys. Rev. Lett. **75**, 4496 (1995).

[17] A. MacKinnon and B. Kramer, Phys. Rev. Lett. **47**, 1546 (1981); B. Kramer and A. MacKinnon, Rep. Prog. Phys. **56**, 1469 (1993).

[18] Y. Imry, Europhys. Lett. **1**, 249 (1986).

[19] P.A. Mello and J.L. Pichard Phys. Rev. B **40**, 5276 (1989); J.L. Pichard, In: *Quantum coherence in Mesoscopic systems*, Ed.: B. Kramer, NATO ASI Series, Series B: Physics **254**, 369 (Plenum Press, N.Y., 1992).